INSTITUTE OF PHYSICS PUBLISHING SEMICONDUCTOR SCIENCE AND TECHNOLOGY

Semicond. Sci. Technol. **20** (2005) S300–S306 doi:10.1088/0268-1242/20/7/022

Two-dimensional photonic crystal slabs in parallel-plate metal waveguides studied with terahertz time-domain spectroscopy

Zhongping Jian, Jeremy Pearce and Daniel M Mittleman

Department of Electrical and Computer Engineering, Rice University, MS-366, 6100 Main St, Houston, TX 77005, USA

E-mail: daniel@rice.edu

Received 30 March 2005
Published 8 June 2005
Online at stacks.iop.org/SST/20/S300

Abstract

In this paper, we report our experimental study on two-dimensional photonic crystal slabs embedded inside parallel-plate metal waveguides, using terahertz time-domain spectroscopy. We observe that the temporal response of the photonic crystal slabs is significantly dispersed, indicative of strong dispersion near the edges of the photonic band gap. In the frequency domain, we observe several gaps whose sizes compare well with those from transfer matrix calculations. The group velocity and group velocity dispersion are characterized using a short-time Fourier transform analysis, and the results are consistent with the predictions from the photonic band structure. We have also measured reflection spectra using the photonic crystal as a 90° turning mirror, and in this way demonstrated frequency-selective components for quasi-optic guided wave propagation of terahertz pulses.

(Some figures in this article are in colour only in the electronic version)

1. Introduction

Much interest in terahertz (THz) radiation has been inspired recently by demonstrations of a variety of possible applications [1]. In particular, THz techniques offer the possibility for extremely broadband and secure communication channels. For these and other uses, new methods for manipulation of terahertz signals are required. One promising candidate is photonic crystals. Photonic crystals are materials that exhibit periodicity in the dielectric function in one or more dimensions [2, 3]. Because of the spatial periodicity, the dispersion relation for electromagnetic radiation, $\omega = ck/\sqrt{\varepsilon}$, is modified. Certain frequencies of light may be forbidden to propagate in certain directions, leading to a gap in the photon density of states. By selectively disrupting the dielectric periodicity, one can introduce propagating modes into these gaps. This effect can be exploited for switching, adding or dropping wavelength channels, or multiplexing operations. Such localized modes can also be the basis for wavelength-scale cavities and novel compact waveguide structures [4].

Although the majority of work on photonic crystals has been directed towards their eventual use at telecommunications wavelengths, there have been several examples of terahertz photonic crystals. Initially, these studies were motivated by the desire to understand the optics of periodic media. Larger structures, designed for longer wavelengths, can act as useful models of the behaviour to be expected when the equivalent design is fabricated for shorter wavelengths. Both two-dimensional [5, 6] and three-dimensional [7–13] photonic crystals have been described. Recently, the value of optical components specifically for THz applications has become a more compelling factor, leading to an increasing interest in the THz properties of periodic systems [14–23].

In this work, we focus our interests on two-dimensional photonic crystals, of the type most commonly envisioned for optical telecommunications applications. The specific design, illustrated in figure 1, consists of a hexagonal lattice of air holes in a dielectric slab. In this photonic crystal, propagating waves are confined in two dimensions by the periodic modulation of the dielectric, and in the third by conventional waveguiding. The use of this geometry is motivated by several factors. First, it is among the most thoroughly studied photonic crystal systems [24]. We can take inspiration from these earlier works for the design of specific waveguide or resonator structures.

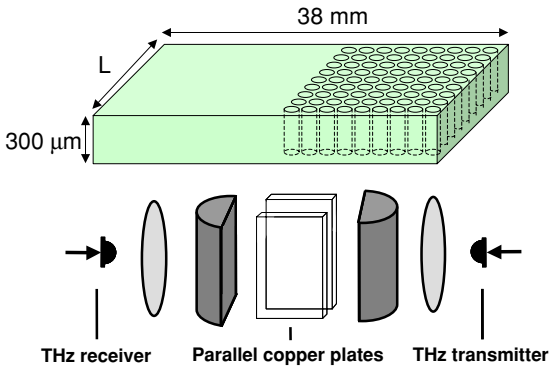

Figure 1. Top: a schematic of the photonic crystal slab, consisting of an array of holes etched through a 300 μm thick silicon wafer. Only half of the area of the wafer is etched, so that the unetched portion can be used as a reference. Bottom: a schematic of the optics used to couple the THz radiation into and out of the parallel-plate metal waveguide, into which the photonic crystal can be inserted. The polarization of the THz beam is perpendicular to the plane of the slabs, so only TM modes are excited.

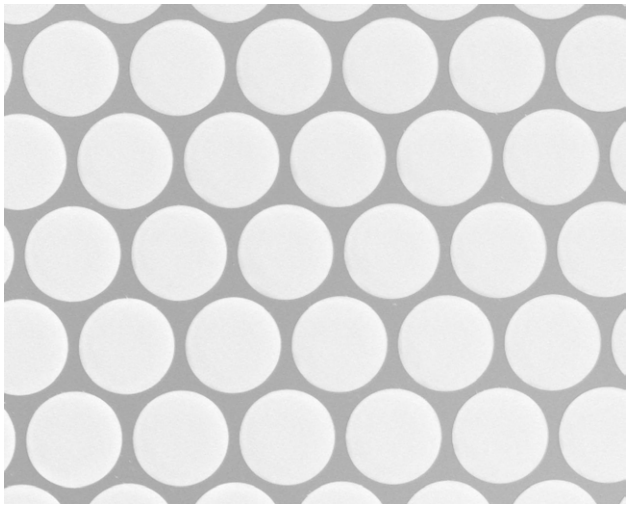

Figure 2. A top-down image of a portion of one sample fabricated using deep reactive ion etching, as described in the text. In this image, the diameter of the air holes is 360 μm.

Second, this planar design permits us to exploit recent advances in terahertz quasi-optic waveguide development. In a series of recent experiments, Grischkowsky and co-workers have demonstrated low-loss, low-dispersion guiding of single-cycle terahertz pulses in parallel-plate metal waveguides [25–27]. By sandwiching a patterned dielectric slab between two parallel metal plates, we can achieve guiding in a system for which the only significant attenuation and dispersion arise from the photonic band structure. This unique configuration permits the direct study of the transmissive and dispersive properties of photonic crystal structures, without the need to correct for the loss or dispersion associated with the planar waveguide.

Here, we describe the characterization of a two-dimensional photonic crystal using terahertz time-domain spectroscopy (THz-TDS) [28, 29]. Comparing with other techniques, THz-TDS has its own advantages, especially in the characterization of dispersion properties. To date, most of these investigations use interferometric techniques [30–33], which compare the pulse transmitted through a photonic crystal and a reference pulse. These methods could be challenging if the transmitted pulse is substantially reshaped, due to the nature of the correlation method. However, in a terahertz time-domain spectroscopy system, one measures $E(t)$ with a temporal resolution which is less than one cycle of the optical field. As a result, pulse reshaping and chirp can be characterized with very high accuracy. Using THz-TDS, we have directly measured both the amplitude and phase of the transmitted radiation, along two different high symmetry axes of the crystal. These results are compared to simulations based on a transfer matrix method [34, 35]. By displaying the results on a time–frequency plot, we can directly visualize the dispersive characteristics near the edges of photonic band gaps. These results can be obtained both in transmission and in 90° reflection, in a quasi-optic-coupled planar waveguide.

2. Experiment

A schematic representation of the experimental set-up is shown in figure 1 [23]. Broadband single-cycle terahertz pulses are generated and detected using ultrafast photoconductive antennas. The terahertz radiation is first collimated and then focused into the waveguide by a plano-cylindrical lens. An identical set-up is used at the output facet to collect the transmitted radiation. The waveguide consists of two parallel copper plates, which provide a nearly perfect metallic boundary for the guided wave. When the electric field of the input pulse is linearly polarized in the direction perpendicular to the plane of the plates, only the TM modes are excited inside the waveguide. The spacing between the waveguide plates is kept fixed at 300 μm.

The photonic crystal slabs consist of a hexagonal array of circular holes etched all the way through a 300 μm thick high-resistivity silicon wafer, using deep reactive ion etching [21]. The holes have vertical sidewalls with diameters of 360 μm, and the lattice has a pitch of 400 μm. High-resistivity (greater than 10^4 Ω cm) silicon is chosen because the absorption is low enough to be negligible, and the refractive index is essentially dispersionless ($n = 3.418$) over the entire bandwidth of the THz pulses [36]. This index contrast (silicon versus air) is large enough to open a sizeable complete band gap for both TE and TM polarizations. In the long wavelength limit, the photonic crystal behaves like a homogeneous dielectric with a refractive index of 1.96, the volume-weighted average. We have prepared one sample with 4 unit cells for propagation along the Γ–K direction, and three additional samples with 5, 10, and 20 unit cells oriented along the Γ–M direction. As shown schematically in figure 1, each has been etched over only half of the area of the wafer. We may use either the unetched portions or simply an air-filled waveguide as a reference for our transmission measurements. A top-down image of a portion of one sample is shown in figure 2.

3. Results and discussion

3.1. Band structures

Using an available software package based on the plane-wave expansion method, we calculate the band structures for TM

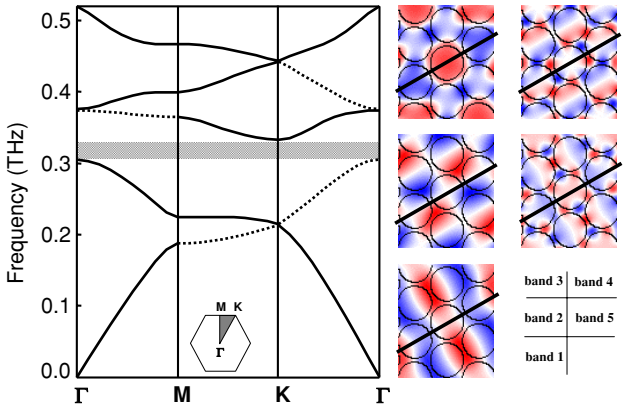

Figure 3. Left: band structure for TM modes of the photonic crystal, with infinite thickness in the direction parallel to the axes of the air holes. This is computed using a plane-wave expansion method [37, 38]. A complete band gap is denoted by the grey region. Dotted lines represent bands whose fields are anti-symmetric with respect to the Γ–K direction, and which therefore cannot be efficiently excited by the symmetric input field [5, 6]. The inset shows the two-dimensional Brillouin zone, with high symmetry points labelled. Right: vertical components of the electric fields for bands between the Γ and K points. Those of bands 1, 3 and 5 are symmetric with respect to the Γ–K direction (denoted by the black line), while those of bands 2 and 4 are anti-symmetric. The key at the lower right indicates which image corresponds to each band. This figure is best appreciated in colour in the electronic web version of this article.

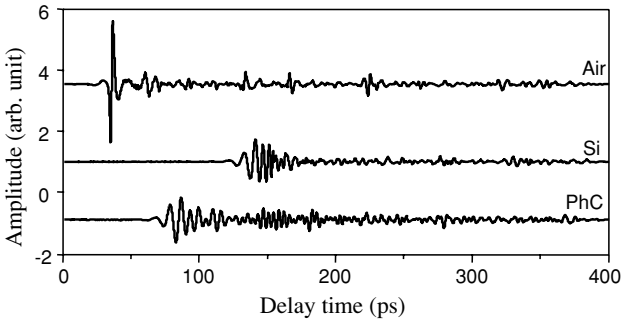

Figure 4. Typical measured time-domain waveforms, for the situations when the metal waveguide is filled with air, silicon and the photonic crystal slab, from top to bottom, respectively. The air signal shows no dispersion, and the silicon signal shows a little dispersion resulting from multimode excitation of the waveguide. The photonic crystal signal is significantly dispersed, extending to hundreds of picoseconds. This dispersion results from the band structure of the photonic crystal, in particular near the edges of the band gap.

modes of our photonic crystal, assuming the thickness of the photonic crystal slab to be infinite [37, 38]. We note that the finite thickness of the slab leads to systematic shifts between the calculation and the experiment, as detailed further below. The calculated band structures are shown in the left side of figure 3. A complete gap is predicted between 0.30 and 0.33 THz. At the right side, we show the calculated vertical (parallel to the centre axis of air holes) component of the electric field, for the lowest five bands between the Γ and K points. Since the input fields are TM polarized, the vertical component is the only non-zero part of the electric field. As can be seen, the fields of bands 1, 3 and 5 are symmetric with respect to the Γ–K direction (denoted by the black lines), while those of bands 2 and 4 are anti-symmetric. Since the input waves are symmetric, these anti-symmetric bands cannot be efficiently excited by the input field. Thus, although the complete band gap covers only a small region of frequency, we expect much larger regions of low transmission due to uncoupled modes [5, 6]. In the band structure diagram, the uncoupled modes are shown as dashed lines, indicating the larger regions of low transmission. For example, the apparent gap along the Γ–K direction extends from 0.22 to 0.33 THz, although only the high-frequency portion of this region corresponds to the complete gap. A similar analysis for the Γ–M direction indicates that band 3 is an anti-symmetric (uncoupled) band in that direction.

3.2. Time-domain waveforms

Figure 4 shows several typical detected waveforms, measured in transmission through the waveguide. When there is no silicon wafer inside the waveguide, we detected a single-cycle terahertz pulse consistent with the previously reported results on parallel-plate metal waveguides [26, 39]. The small irregular oscillations which follow the main pulse are characteristic of the system response of the THz spectrometer, arising from electrical and optical reflections. When the unetched silicon slab is inserted into the waveguide, the pulse is no longer a single cycle. This dispersion results mainly from multimode propagation inside the waveguide. When the high-index material is placed inside the waveguide at the fixed separation of 300 μm, it is possible for the incoming wave to excite not only the TM_0 (TEM) mode, but also several higher even-parity TM modes [40]. Odd-parity modes cannot be excited by the input beam, and so do not contribute. Since these TM_n modes each have different propagation constants, the result is a net dispersion of the THz pulse.

When the photonic crystal is placed into the waveguide, a much larger dispersion results. In contrast to the case of the solid silicon wafer, this is primarily *not* due to waveguide dispersion. The lower average index of the photonic crystal pushes the cutoff frequency of higher order TM modes to larger frequencies. As a result, a second even-parity waveguide mode (the TM_2 mode) is only excited by spectral components in the high-frequency portion of the THz pulse spectrum where the spectral intensity is quite low. Instead, the dispersion is primarily the result of the dispersive effects of the photonic band structure, discussed further below. Incidentally, the effect of the lower average index can also be seen in the transit time of the earliest arriving portion of the THz signal through the waveguide, intermediate between the cases of air and solid silicon. As we have noted before [23], the maximum of this earliest arriving signal can be used to estimate the effective refractive index of the photonic crystal structure. The result is in good agreement with the value computed using the known filling fraction of the sample.

3.3. Frequency response

In order to characterize the effects of band gaps and uncoupled modes, we plot in figures 5 and 6 the normalized transmission spectra in the frequency domain. Figure 5(*a*) shows the transmission coefficient of the sample in the Γ–K direction, relative to those of an air-filled waveguide. Two

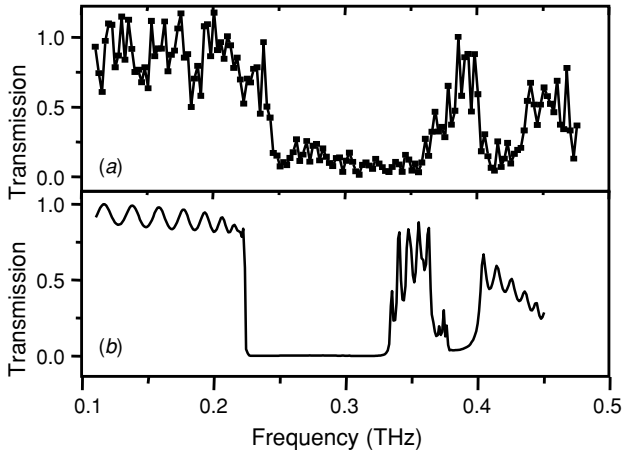

Figure 5. (*a*) Measured power transmission spectrum of the photonic crystal inside the metal waveguide, for the Γ–K direction, along which the sample has 4 unit cells. This is computed using the Fourier transforms of the time-domain waveforms, with the air-filled guide as a reference. (*b*) Γ–K transmission spectrum computed using a transfer matrix method, for comparison with the experimental result. The comparison is quite good, except for a systematic redshift of about 0.025 THz, attributed to the finite thickness of the photonic crystal, which is not considered in the numerical calculation.

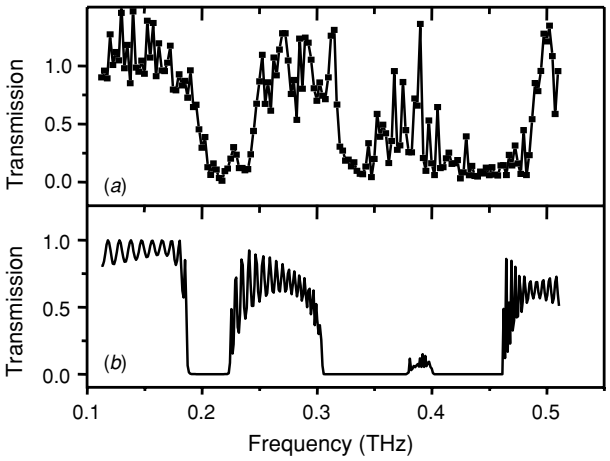

Figure 6. (*a*) Measured power transmission spectrum of the photonic crystal inside the metal waveguide, for the Γ–M direction, along which the sample has 10 unit cells. This is computed using the Fourier transforms of the time-domain waveforms, with the air-filled guide as a reference. (*b*) Γ–M transmission spectrum computed using a transfer matrix method, for comparison with the experimental result. A redshift of the theory with respect to the experiment is observed, similar to the results of figure 5.

low-transmission regions can be observed. For comparison, we also compute the transmission spectrum using a transfer matrix method [34], which again assumes an infinite thickness for the photonic crystal slab. The result, as shown in figure 5(*b*), shows almost the same gap widths as those from the experimental result, except there is a systematic redshift of about 0.025 THz. This shift has previously been attributed to the finite thickness of the photonic crystal slab [21, 24, 41]. Interestingly, the experimental transmission in the first gap is somewhat larger at the low-frequency side of the gap (near 0.27 THz) than it is at the high-frequency side (near 0.32 THz). This difference may be due to the fact that only the higher frequency portion of this region corresponds to the complete photonic band gap, while the lower portion corresponds to the region of uncoupled modes. A small residual amount of radiation may be coupled into these modes due to imperfections in the wave front of the focused THz pulse, leading to a slightly higher transmission coefficient. This phenomenon is also seen in the second gap (near 0.42 THz), which also results from the anti-symmetric modes, and has transmission coefficients of the same order as those for the low-frequency portion of the first gap. We note that the transmission coefficients in the region of the complete gap are not as small as the theoretically computed transmission. This residual transmission reflects the noise floor of the measurement.

Figure 6 shows the measured and calculated transmission coefficients for the Γ–M direction. Once again, we observe a similar degree of correspondence between the two results, along with a similar redshift due to the finite thickness of the photonic crystal.

3.4. Group velocity

As noted above, propagation through the photonic crystal leads to substantial dispersion of the time-domain waveforms, due to the strong group velocity dispersion associated with the band structure. This dispersion can be used for ultrafast pulse manipulation, including for example pulse compression [42, 43] and optical delay lines [44, 45]. There have been a few reports on using ultrafast pulses to probe the dispersion at or near the band gaps of photonic crystals by measuring the difference of arrival times between one pulse transmitted through a photonic crystal and the other through a reference sample [46–49]. Others have used interferometric techniques, comparing the pulse transmitted through a photonic crystal and a reference pulse [30–33]. Direct measurements of pulse group velocity have also been realized using non-linear effects [50, 51].

Here, we take advantage of the coherent nature of the THz-TDS measurement to investigate the dispersion associated with the photonic band structure. Because this technique permits sub-cycle temporal resolution of the electric field, even strongly distorted or chirped terahertz pulses can be accurately characterized. Since the bandwidth of our terahertz pulse is much broader than the size of the stop-gap, it permits us to extract information over a broad spectral range, giving a complete description of the properties of photonic crystals in the frequency range of interest.

To better illustrate the effects of dispersive propagation, we present the measured signals in both time and frequency domains. We accomplish this using a short-time Fourier transform (STFT) [52, 53]. This procedure is widely used for time–frequency analysis of non-stationary signals. In STFT, the signal is multiplied by a window function, and is then Fourier analysed to determine the spectral content of the signal within the specified window. By sliding the window along the signal, one obtains the temporal evolution of the frequency content. The spectrogram computed in this way can be represented as

$$S(\omega, t) = \int_{-\infty}^{+\infty} f(\tau) w(\tau - t)\, \mathrm{e}^{-\mathrm{i}\omega\tau}\, \mathrm{d}\tau$$

where $f(\tau)$ is the measured waveform and $w(\tau - t)$ is a

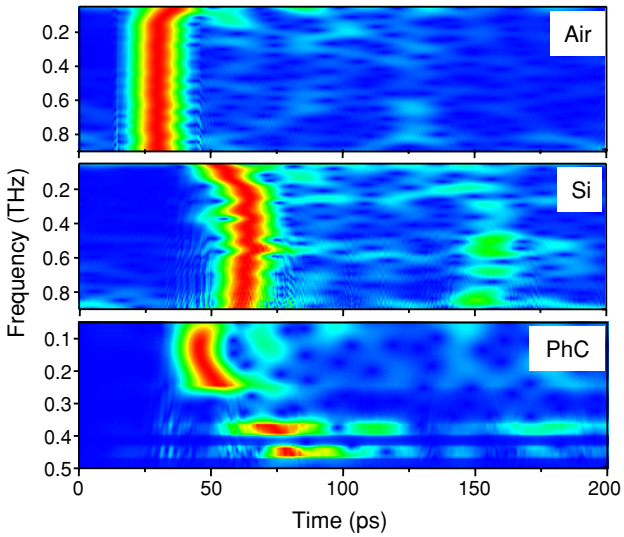

Figure 7. Short-time Fourier transform plots of typical waveforms for air, silicon, and photonic crystal samples. Here, red indicates high amplitude and blue indicates low amplitude. In the upper plot, the air-filled waveguide is dispersionless, so all of the spectral components of the THz pulse arrive at the same time. In the middle plot, the small dispersive effects arise from multimode excitation of the waveguide. In the lower plot, large dispersion is observed near the edges of the band gaps in the photonic crystal. The photonic crystal signal is for propagation along the Γ–K direction. This figure is best appreciated in colour in the electronic web version of this article.

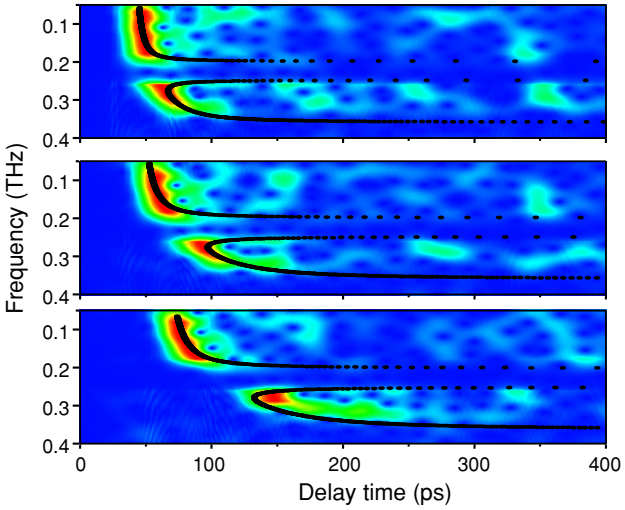

Figure 8. Short-time Fourier transform plots of the THz pulses transmitted through three different samples along the Γ–M direction. In these samples, the thicknesses are 5, 10 and 20 unit cells, from top to bottom, respectively. As a result of the increasing propagation distance inside the dispersive medium, both the transit times and the dispersion increase. The solid black lines are calculated as described in the text. These are plotted using only one adjustable parameter: the frequency shift due to the finite thickness of the crystal, mentioned in the context of figures 5 and 6. This parameter is the same for all three panels. This figure is best appreciated in colour in the electronic web version of this article.

Hamming window centred at t. The duration of the window function determines the time and frequency resolution. Here, we choose the duration to be 30 ps, which gives a frequency resolution of 0.03 THz. In order to display the results, we first normalize each spectral component of $S(\omega, t)$ of the photonic crystal data to that of the corresponding frequency in the spectrogram of the waveform taken with an empty waveguide. Then, in order to avoid dynamic range problems in the false-colour plot for the photonic crystal data, we normalize $S(\omega, t)$ at each frequency by dividing by the maximum value for that frequency. If, for certain values of frequency, the maximum value is smaller than a critical value, which we set as 10% of the maximum value among all those maximum values, this is an indication that this frequency falls within a stop band, and the normalization factor is increased accordingly. The threshold value of 10% is chosen based on the experimental transmission spectra (e.g. figures 5 and 6). It permits us to clearly distinguish between spectral regions inside and outside of the stop bands.

The spectrograms computed in this way are shown in figure 7. All frequency components in the air signal emerge from the waveguide at almost the same time, indicative of zero dispersion. For the silicon signal, the transit times vary slightly due to the aforementioned multimode excitation of the waveguide. In contrast, both the band gaps and the striking dispersion of the photonic crystal signal become very clear in this false-colour plot. Similar results for propagation along the Γ–M direction are shown in figure 8. Here, spectrograms are displayed for the three different photonic crystal samples, identical except for the propagation lengths.

We can directly compare these results with the computed band structure. For light propagating in a given band, the transit time through the photonic crystal can be expressed as

$$\Delta t(\omega) = \frac{L}{v_g(\omega)}$$

where L is the length of the slab and the group velocity $v_g(\omega)$ is calculated numerically from the band structure using the Hellman–Feynman theorem [37]. The transit times computed in this fashion, for Γ–M, are shown as black curves superimposed on figure 8. The computed curves have been shifted along the frequency axis, to account for the finite thickness frequency shift mentioned above, in the context of figures 5 and 6. In addition, the calculated results must be shifted along the time axis, since in these measurements the zero of the time is arbitrarily chosen. We determine the absolute time shift by referencing the calculations to the zero of time defined by transmission through an air-filled guide (as in figure 7). Thus, apart from the aforementioned finite thickness frequency shift, the black curves in these plots are computed with no adjustable parameters. The correspondence is extremely good, indicating the high quality of the photonic crystals which can be fabricated for THz applications.

3.5. Reflection spectra

Using terahertz time-domain techniques, it is also generally possible to measure reflection spectra. However, in the present case, this presents a special challenge. Because we are coupling terahertz waves from free space into the waveguide, it is difficult to couple 100% of the input beam into the waveguide. Part of the beam is inevitably reflected from the copper plates above or below the dielectric slab. This reflected beam can be significant compared with the reflection from the thin photonic crystal slab. Because the two reflections

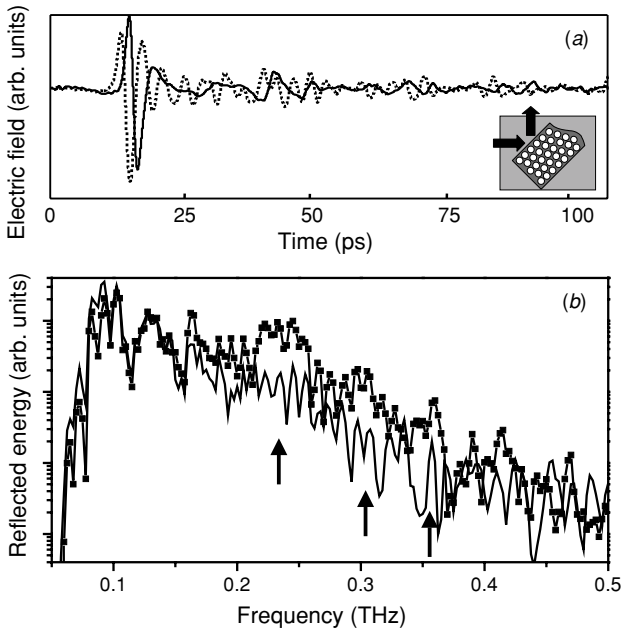

Figure 9. Upper: time-domain waveforms reflected from an unpatterned silicon reference slab (solid) and a photonic crystal (dotted). The inset shows a schematic of the reflection geometry. In these measurements, the Γ–M direction is perpendicular to the incident surface of the photonic crystal. Lower: the power spectra of the two waveforms shown in the upper plot, on a log scale. The photonic crystal result (squares) exhibits enhanced reflection in certain spectral regions (indicated by arrows), due to the high reflectivity of band gap regions.

overlap in the time domain, it can be difficult to experimentally distinguish them from each other. So, instead of measuring the reflected beam at normal incidence, we employ a 90° set-up, as shown in the inset of figure 9. Here, the photonic crystal is used inside the metal waveguide as a quasi-optic turning mirror [27]. We obtain a reference signal by replacing the photonic crystal with a silicon slab of the same thickness. Typical detected waveforms are shown in figure 9(*a*), where the reference signal keeps its single-cycle property while the signal reflected by the photonic crystal slab is significantly extended in duration. We then calculate the power spectra via Fourier transform of the two measured signals. The results are shown in figure 9(*b*). We observe that, in certain spectral regions near the complete band gap, the reflection from the photonic crystal is significantly enhanced relative to that from the un-patterned silicon wafer. This result demonstrates that photonic crystals can be used in combination with quasi-optics for a variety of functions such as frequency selection and pulse shaping.

4. Conclusion

In conclusion, we have studied the optical properties of two-dimensional photonic crystal slabs with copper claddings, using terahertz time-domain spectroscopy. The transmission coefficients in the frequency domain match well to those from transfer matrix calculations, except that there is a systematic shift of the band edges due to finite thickness effects. Using short-time Fourier transform, we can display the data in both time and frequency domains, which gives a useful intuitive picture of the propagation characteristics near the band edges. We can also measure reflection spectra, and in this way construct frequency-selective components for quasi-optic guided wave propagation of terahertz pulses. Such components are in principle tunable by varying the angle of the photonic crystal slab. Finally, we note that the long wavelength (compared to visible and near-infrared optics) permits the easy fabrication of photonic crystals, which are essentially ideal, with no defects or disorder of any kind. As a result, these experiments are extremely well described by theoretical models, and it may be possible to observe subtle effects which would otherwise be obscured by the disorder present in less perfect samples.

Acknowledgment

The authors would like to thank Andrew L Reynolds for providing Transfer Matrix Method codes to compute transmission coefficients. This work is supported in part by the National Science Foundation.

References

[1] Mittleman D M (ed) 2003 *Sensing with Terahertz Radiation (Springer Series in Optical Sciences)* (Heidelberg: Springer)
[2] Yablonovitch E 1987 Inhibited spontaneous emission in solid-state physics and electronics *Phys. Rev. Lett.* **58** 2059
[3] John S 1987 Strong localization of photons in certain disordered dielectric superlattices *Phys. Rev. Lett.* **58** 2486–9
[4] Joannopoulos J D, Meade R D and Winn J N 1995 *Photonic Crystals : Molding the Flow of Light* (Princeton: Princeton University Press)
[5] Robertson W M, Arjavalingam G, Meade R D, Brommer K D, Rappe A M and Joannopoulos J D 1992 Measurement of photonic band structure in a two-dimensional periodic dielectric array *Phys. Rev. Lett.* **68** 2023
[6] Wada M, Sakoda K and Inoue K 1995 Far-infrared spectroscopy study of an uncoupled mode in a two-dimensional photonic lattice *Phys. Rev.* B **52** 16297
[7] Ozbay E, Michel E, Tuttle G, Biswas R, Ho K M, Bostak J and Bloom D M 1994 Terahertz spectroscopy of three-dimensional photonic band-gap crystals *Opt. Lett.* **19** 1155
[8] Ozbay E, Michel E, Tuttle G, Biswas R, Sigalis M and Ho K-M 1994 Micromachined millimeter-wave photonic band-gap crystals *Appl. Phys. Lett.* **64** 2059
[9] Ozbay E 1996 Layer-by-layer photonic crystals from microwave to far-infrared frequencies *J. Opt. Soc. Am.* B **13** 1945
[10] Wanke M C, Lehmann O, Müller K, Wen Q and Stuke M 1997 Laser rapid prototyping of photonic band-gap microstructures *Science* **275** 1284
[11] Chelnokov A, Rowson S, Lourtioz J-M, Duvillaret L and Coutaz J-L 1997 Terahertz characterization of mechanically machined 3D photonic crystal *Electron. Lett.* **33** 1981
[12] Aoki T, Takeda M W, Haus J W, Yuan Z, Tani M, Sakai K, Kawai N and Inoue K 2001 Terahertz time-domain study of a pseudo-simple-cubic photonic lattice *Phys. Rev.* B **64** 045106
[13] Feiertag G, Ehrfeld W, Freimuth H, Kolle H, Lehr H, Schmidt M, Sigalis M M, Soukoulis C M, Kiriakidis G, Pedersen T, Kuhl J and Koenig W 1997 Fabrication of photonic crystals by deep x-ray lithography *Appl. Phys. Lett.* **71** 1441

[14] Gadot F, de Lustrac A, Lourtioz J-M, Brillat T, Ammouche A and Akmansoy E 1999 High-transmission defect modes in two-dimensional metallic photonic crystals *J. Appl. Phys.* **85** 8499
[15] Jin C, Cheng B, Li Z, Zhang D, Li L-M and Zhang Z-Q 1999 Two dimensional metallic photonic crystal in the THz range *Opt. Commun.* **166** 9
[16] Temelkuran B, Bayindir M, Ozbay E, Kavanaugh J P, Sigalas M M and Tuttl G 2001 Quasimetallic silicon micromachined photonic crystals *Appl. Phys. Lett.* **78** 264
[17] Gonzalo R, Ederra I, Mann C M and Maagt Pd 2001 Radiation properties of terahertz dipole antenna mounted on photonic crystal *Electron. Lett.* **37** 613
[18] Kitahara H, Tsumura N, Kondo H, Takeda M W, Haus J W, Yuan Z, Kawai N, Sakoda K and Inoue K 2001 Terahertz wave dispersion in two-dimensional photonic crystals *Phys. Rev.* B **64** 045202
[19] Han H, Park H, Cho M and Kim J 2002 Terahertz pulse propagation in a plastic photonic crystal fiber *Appl. Phys. Lett.* **80** 2634
[20] Wang S-W, Lu W, Chen X-S, Li Z-F, Shen X-C and Wen W 2003 Two-dimensional photonic crystal at THz frequencies constructed by metal-coated cylinders *J. Appl. Phys.* **93** 9401
[21] Jukam N and Sherwin M S 2003 Two-dimensional terahertz photonic crystal fabricated by deep reactive ion etching in Si *Appl. Phys. Lett.* **83** 21
[22] Drysdale T D, Blaikie R J and Cumming D R S 2003 Calculated and measured transmittance of a tunable metallic photonic crystal filter for terahertz frequencies *Appl. Phys. Lett.* **83** 5362
[23] Jian Z, Pearce J and Mittleman D M 2004 Defect modes in photonic crystal slabs studied using terahertz time-domain spectroscopy *Opt. Lett.* **29** 2067
[24] Johnson S G, Fan S, Villeneuve P R, Joannopoulos J D and Kolodziejski L A 1999 Guided modes in photonic crystal slabs *Phys. Rev.* B **60** 5751
[25] Mendis R and Grischkowsky D 2000 Plastic ribbon THz waveguide *J. Appl. Phys.* **88** 4449
[26] Mendis R and Grischkowsky D 2001 Undistorted guided-wave propagation of subpicosecond terahertz pulses *Opt. Lett.* **26** 846
[27] Coleman S and Grischkowsky D 2003 A THz transverse electromagnetic mode two-dimensional interconnect layer incorporating quasi-optics *Appl. Phys. Lett.* **83** 3656
[28] Smith P R, Austo D H and Nuss M C 1988 Subpicosecond photoconducting dipole antennas *IEEE J. Quantum Electron.* **24** 255
[29] van Exter M and Grischkowsky D 1990 Characterization of an optoelectronic terahertz beam system *IEEE Trans. Microw. Theory Tech.* **38** 1684–91
[30] Tarhan I I, Zinkin M P and Watson G H 1995 Interferometric technique for the measurement of photonic band structure in colloidal crystals *Opt. Lett.* **20** 1571
[31] Imhof A, Vos W L, Sprik R and Lagendijk A 1999 Large dispersive effects near the band edges of photonic crystals *Phys. Rev. Lett.* **83** 2942
[32] Gersen H, Korterik J P, van Hulst N F and Kuipers L 2003 Tracking ultrashort pulses through dispersive media: experiment and theory *Phys. Rev.* E **68** 026604
[33] Galli M, Bajoni D, Marabelli F, Andreani L C, Pavesi L and Pucker G 2004 Photonic bands and group-velocity dispersion in Si/SiO_2 photonic crystals from white-light interferometry *Phys. Rev.* B **69** 115107
[34] Pendry J B and MacKinnon A 1992 Calculation of photon dispersion relations *Phys. Rev. Lett.* **69** 2772
[35] TMM software supplied by A L Reynolds, University of Glasgow
[36] Grischkowsky D, Keiding S, van Exter M and Fattinger C 1990 Far-infrared time-domain spectroscopy with terahertz beams of dielectrics and semiconductors *J. Opt. Soc. Am.* B **7** 2006–15
[37] MIT Photonic Bands, http://ab-initio.mit.edu/mpb
[38] Johnson S G and Joannopoulos J D 2001 Block-iterative frequency-domain ethods for Maxwell's equations in a planewave basis *Opt. Exp.* **8** 173
[39] Mendis R and Grischkowsky D 2001 THz interconnect with low loss and low group velocity dispersion *IEEE Microw. Wirel. Compon. Lett.* **11** 444
[40] Marcuvitz N 1951 *Waveguide Handbook* (New York: McGraw-Hill)
[41] Whittaker D M, Culshaw J S, Astratov V N and Skolnick M S 2002 Photonic band structure of patterned waveguides with dielectric and metallic cladding *Phys. Rev.* B **65** 073102
[42] Eggleton B J, Lenz G, Slusher R E and Litchinitser N M 1998 Compression of optical pulses spectrally broadened by self-phase modulation with a fiber Bragg grating in transmission *Appl. Opt.* **37** 7055
[43] Andreev A V, Balakin A V, Ozheredov I A, Shkurinov A P, Masselin P, Mouret G and Boucher D 2001 Compression of femtosecond laser pulses in thin one-dimensional photonic crystals *Phys. Rev.* E **63** 016602
[44] Sugimoto Y, Lan S, Nishikawa S, Ikeda N, Ishikawa H and Asakawa K 2002 Design and fabrication of impurity band-based photonic crystal waveguides for optical delay lines *Appl. Phys. Lett.* **81** 1946
[45] Munday J N and Robertson W M 2003 Slow electromagnetic pulse propagation through a narrow transmission band in a coaxial photonic crystal *Appl. Phys. Lett.* **83** 1053
[46] Scalora M *et al* 1996 Ultrashort pulse propagation at the photonic band edge: large tunable group delay with minimal distortion and loss *Phys. Rev.* E **54** 1078
[47] Vlasov Y A, Petit S, Klein G, Honerlage B and Hirlimann C 1999 Femtosecond measurements of the time of flight of photons in a three-dimensional photonic crystal *Phys. Rev.* E **60** 1030
[48] Inoue K, Kawai N, Sugimoto Y, Carlsson N, Ikeda N and Asakawa K 2002 Observation of small group velocity in two-dimensional AlGaAs-based photonic crystal slabs *Phys. Rev.* B **65** 121308
[49] Asano T, Kiyota K, Kumamoto D, Song B-S and Nodab S 2004 Time-domain measurement of picosecond light-pulse propagation in a two-dimensional photonic crystal-slab waveguide *Appl. Phys. Lett.* **84** 4690
[50] Gamble L J, Diffey W M, Cole S T, Fork R L and Jones D K 1999 Simultaneous measurement of group delay and transmission of a one-dimensional photonic crystal *Opt. Express* **5** 267
[51] Netti M C, Finlayson C E, Baumberg J J, Charlton M D B, Zoorob M E, Wilkinson J S and Parker G J 2002 Separation of photonic crystal waveguides modes using femtosecond time-of-flight *Appl. Phys. Lett.* **81** 3927
[52] Mallat S 1999 *A Wavelet Tour of Signal Processing* 2nd edn (San Diego: Academic)
[53] Time–Frequency Matlab Toolbox, http://gdr-isis.org/Applications/tftb/iutsn.univ-nantes.fr/auger/tftb.html